Methanol and Water Dissociation on TiO 2 (110): The Role of Surface Oxygen

ARTICLE *in* THE JOURNAL OF PHYSICAL CHEMISTRY C · OCTOBER 2008

Impact Factor: 4.77 · DOI: 10.1021/jp805759y

THE JOURNAL OF PHYSICAL CHEMISTRY C

Letter

Methanol and Water Dissociation on TiO (110): The Role of Surface Oxygen

Jaime Oviedo, Roci#o Sa#nchez-de-Armas, Miguel A#ngel San Miguel, and Javier F. Sanz

J. Phys. Chem. C, **2008**, 112 (46), 17737-17740 • DOI: 10.1021/jp805759y • Publication Date (Web): 29 October 2008

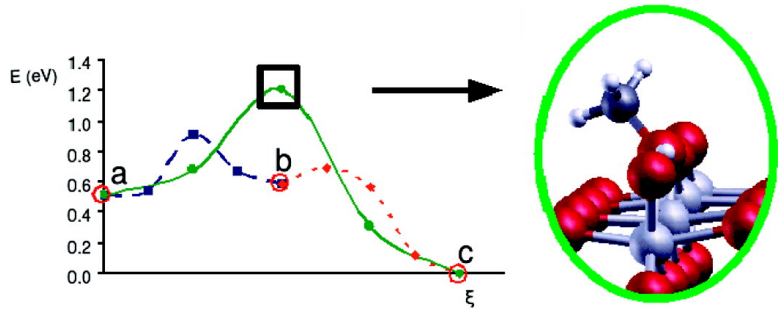

More About This Article

Additional resources and features associated with this article are available within the HTML version:

- Supporting Information
- Access to high resolution figures
- Links to articles and content related to this article
- Copyright permission to reproduce figures and/or text from this article

View the Full Text HTML

THE JOURNAL OF PHYSICAL CHEMISTRY C LETTERS

2008, *112,* 17737–17740
Published on Web 10/29/2008

Methanol and Water Dissociation on TiO_2 (110): The Role of Surface Oxygen

Jaime Oviedo,* Rocío Sánchez-de-Armas, Miguel Ángel San Miguel, and Javier F. Sanz

Department of Physical Chemistry, University of Sevilla, 41012-Sevilla, Spain

Received: July 1, 2008; Revised Manuscript Received: September 24, 2008

Dissociation mechanisms for methanol and water on stoichiometric and defective TiO_2 (110) surfaces have been clarified from periodic density functional calculations. When the molecules are adsorbed on an oxygen vacancy, the most favorable route to dissociation is an indirect mechanism involving, initially, the formation of an intermediate hydroxyl group on in-plane oxygen, followed by the hydrogen transfer to a neighbor bridging oxygen. Since the transient species lifetime is short, they are difficult to be detected. At variance, dissociation on stoichiometric surfaces proceeds readily through a direct hydrogen transfer process from the adsorbate to bridging oxygen. However, the energy barrier for the recombination is low and the species can return to the initial state.

The TiO_2 (110) surface has received considerable attention in the literature due to its utility in studying catalytic and photocatalytic reactions, and it has become a prototype of a metal oxide surface.[1] The most prominent feature on this surface is the presence of under-coordinated oxygen atoms in the outermost layer (Figure 1). These oxygen atoms are called bridging oxygen and can be easily removed to introduce defects (ca. 10%) on the surface.[1] It has been shown that these vacancies act as preferential adsorption sites on the surface.[2−5] In addition, the upper layer is formed by titanium atoms, and also by in-plane oxygen atoms, which have usually been regarded as inactive centers (Figure 1).

The oxidation of alcohols on TiO_2 surfaces has been extensively studied as a model for the catalytic oxidation of organic contaminants.[3,6−14] In a previous work the adsorption and dissociation of methanol molecules on both stoichiometric and defective surfaces was studied and the adsorption was found to be more stable on defects.[5] For the stoichiometric surface, the molecular and dissociated states are almost degenerate and neither state is clearly favored. Although the transition barrier was not explicitly calculated, it was supposed to be small since molecular dynamic (MD) simulations performed at moderate temperatures showed easy interconversion between these states. It is worth noting that a similar situation is found for water, where there is still a long running theoretical controversy about whether water dissociation is energetically feasible on the perfect surface.[15−17] On the other hand, methanol dissociation on a bridging vacancy was found to be favored by ca. 0.5 eV giving rise to a hydroxyl group on a bridging atom (OH_b). However, in this case, MD simulations performed under similar conditions did not show dissociation, thus suggesting that a higher barrier would presumably be involved.

There is already direct STM evidence that alcohols[3,6,7] deprotonate at bridging vacancies with the alkoxy group filling the vacancy and the proton producing an OH_b on a neighboring bridging oxygen. This also holds for water, and the dissociation in this case gives rise to two hydroxyl groups in adjacent bridging sites.[2−4,15,18,19] These measurements are carried out on a time scale of seconds or minutes so it is not possible to infer details on the dissociation mechanism at an atomistic level. The increasing computational resources make it possible to complement the experimental work with theoretical calculations that allow us to find equilibrium geometries and transition states in a reliable way. In this paper, we present a study of the elementary steps involved in the methanol dissociation, including transition state barriers, on both stoichiometric and defective TiO_2 (110) surfaces. The study has been extended to water that is ubiquitously found on this surface[15] and also dissociates through an O−H bond breaking.

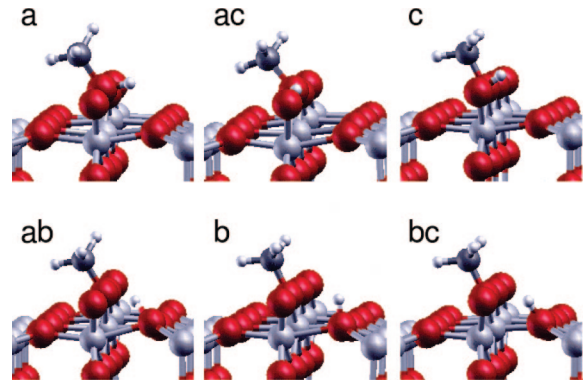

Figure 1. Stationary point and transition state geometries for methanol adsorbed on the defective surface. (a) Molecular state, (b) dissociated on O_{in} state, and (c) dissociated on O_{br} state. The three transition state geometries (ab), (ac), and (bc) are shown. Geometries correspond to six layer slabs and 4 × 2 supercell calculations.

In the present work, the implementation of density functional theory (DFT) with plane waves and the PAW (plane augmented waves) potentials has been used.[20] We chose the generalized gradient approximation (GGA) due to Perdew et al.[21] for the exchange-correlation energy. The calculations were performed with the VASP (Vienna ab initio simulation package) code.[22] For oxygen and carbon, the core only consists of 1s states

* To whom correspondence should be addressed. E-mail: jol@us.es.

10.1021/jp805759y CCC: $40.75

TABLE 1: Relative Energies (eV) for Methanol and Water Molecularly and Dissociatively Adsorbed on the Stoichiometric and Defective Surfaces[a]

	methanol		water	
	stoi.	def.	stoi.	def.
a	0.00	0.50, 0.51, 0.42	0.00	0.49, 0.49, 0.39
b	0.65	0.50, 0.58, 0.50	0.75	0.49, 0.57, 0.49
c	0.02	0.00, 0.00, 0.00	0.14	0.00, 0.00, 0.00

[a] States are labelled as (a) molecular state, (b) dissociated on O_{in} state, and (c) dissociated on O_{br} state. Zero energy is arbitrarily set for the most stable state. For the defective surface data correspond from left to right to four and six layer slabs (4 × 1 supercell) and six layer slabs (4 × 2 supercell).

whereas for Ti, up to and including the 3p shells are frozen and the reference state for the potential generation is s^1d^3.

The surface was represented by four and six layers slabs made of 4 × 1 unit cells. For the defective surface we also used a six layer slab made of a 4 × 2 unit cell. This larger supercell allowed assessing the influence of the molecular interaction on the results. The optimized lattice parameters for the (110) surface unit cell are $a = 4.616$ Å, $c = 2.974$ Å, and $u = 0.304$, and they are used throughout the present work and maintained fixed during the atomic positions relaxation.[23] In order to model defective surfaces, one bridging oxygen atom has been removed from the supercell and thus the system represents a surface with a 12.5% oxygen vacancy concentration, close to experimental conditions. On the stoichiometric surface, the site for molecule adsorption is the 5-fold coordinated titanium. On the defective surface, we explore adsorption directly onto the vacancy as shown in Figure 1. A single molecule is placed on one side of the slab, which represents a coverage of $\theta = 0.25$ or 0.125. Dissociated molecules are also included in this study, with the hydrogen atom bound to bridging or in-plane oxygen atoms. Full convergence tests and technical details can be found in previous work.[5,23] Two sets of calculations were performed. First, we carried out static calculations, i.e., geometry optimizations and transition states searching. This set was carried out at a relatively high level of precision that involved a 400 eV energy cutoff and the 2 × 4 × 1 or 2 × 2 × 1 Monkhorst−Pack *k*-points sets for the 4 × 1 or 4 × 2 supercells, respectively.[24] The climbing nudged elastic band (NEB) method was applied to locate transition states, and the minimum energy pathway was constructed, given the initial and the final stationary geometries.[25,26] In general, three images were used to locate each transition state. A typical NEB calculation took about 5 × 10^3 hours CPU time in a supercomputer. In order to analyze dynamical effects and introduce temperature effects, a second set of calculations consisting of MD calculations in the canonical ensemble was carried out. They were also used as a tool to find stationary points by performing simulations at low temperature starting from several initial geometries. The precision for these simulations was lowered to a 300 eV energy cutoff and they were performed at the Γ point of the Brillouin zone. For hydrogen, a fictional mass of 3 uma was used, which allowed a time step of 1 fs.[5]

Adsorption of methanol (water) on the defective surface preferentially takes place at the vacancy, as shown in Figure 1a (2a). Relative adsorption energies for methanol and water on this defective surface are presented in Table 1. It can be seen that dissociation onto a bridging oxygen to produce a hydroxyl group (OH_b) is thermodynamically favored (c. a. 0.5 eV) for both molecules. However, dissociation to form a hydroxyl group onto in-plane oxygen (OH_{in}) is almost degenerate in energy to the molecular adsorption. Results from four- and six- layer slabs models show the same trends and this is indicative of a good convergence with slab thickness. Furthermore the use of the larger 4 × 2 supercell make little difference what shows the molecular interaction is not significative in this case.

TABLE 2: Transition State Barriers (eV) for Dissociation of Methanol and Water on the Stoichiometric and Defective Surface[a]

	methanol		water	
	stoi.	def.	stoi.	def.
ac	0.11	0.77, 0.69, 0.72	0.30	0.32, 0.42, 0.54
ab		0.39, 0.40, 0.40		0.32, 0.35, 0.39
bc		0.06, 0.11, 0.26		0.13, 0.08, 0.31

[a] States are labelled as (a) molecular state, (b) dissociated on O_{in} state, and (c) dissociated on O_{br} state. For the defective surface data correspond from left to right to four and six layer slabs (4 × 1 supercell) and six layer slabs (4 × 2 supercell).

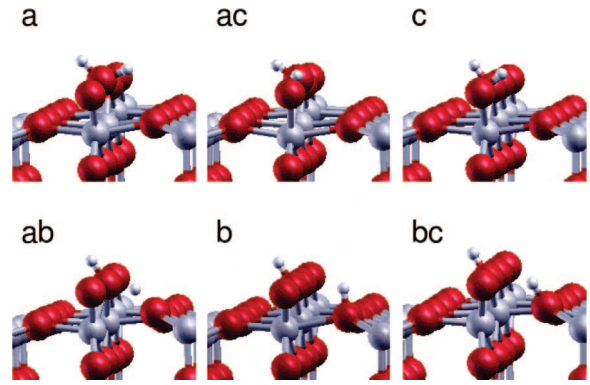

Figure 2. Stationary point and transition state geometries for water adsorbed on the defective surface. (a) Molecular state, (b) Dissociated on O_{in} state, (c) Dissociated on O_{br} state. The three transition state geometries (ab), (ac), and (bc) are shown. Geometries correspond to six layer slabs and 4 × 2 supercell calculations.

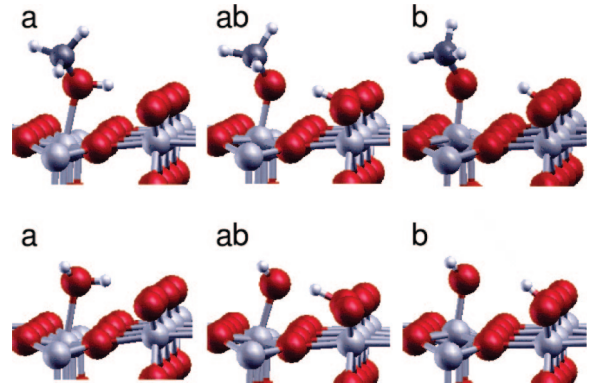

Figure 3. Stationary point and transition state geometries for methanol (left) and water (right) on the stoichiometric surface. (a) Molecular state, (b) Dissociated on O_{br} state. The transition state geometries (ab) are shown. Geometries correspond to six layer slabs and 4 × 1 supercell calculations.

The transition state barriers for a direct transfer of hydrogen from the molecule to bridging oxygen were calculated (Table 2). The barrier was found to be substantially higher for methanol. In order to check the stability of surface species and introduce temperature effects, extensive molecular dynamic calculations were carried out. Remarkably, dissociation was never observed either for methanol or water at temperatures up to 500 K. However, we did observe dissociation onto nearby in-plane

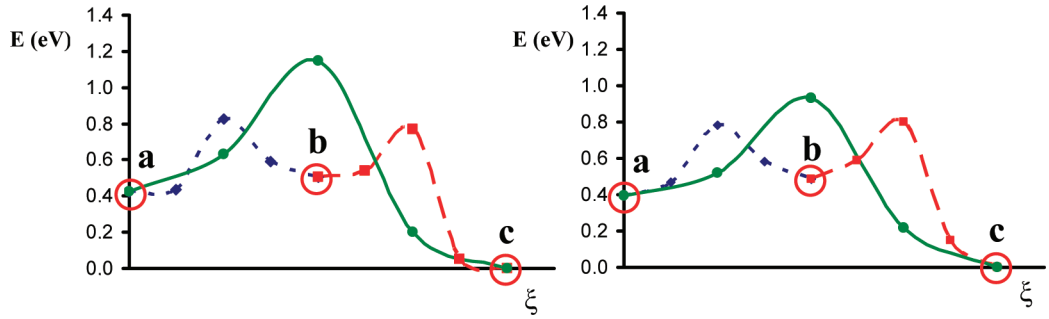

Figure 4. Energy profiles (eV) for dissociation taken from the minimum energy path. Methanol (left) and water (right). Big hollow circles show stationary points with the same notation as in Figures 1 and 2 whereas small full symbols show intermediate images. Paths corresponding to (ab), (bc), and (ac) are represented by dashed, dotted, etc. respectively. The reaction coordinate scales have been modified in order to accommodate three transition barriers per graph.

oxygen in some cases. Inspired by these results a second indirect mechanism was explored, in which the molecule first dissociates transferring a hydrogen atom to an in-plane oxygen so forming an hydroxyl group (OH_{in}), and next, the hydrogen is transferred to the bridging oxygen (Figure 1 and 2).

The transition barriers calculations provided unexpected results since barriers for the two step mechanism are lower than that for the direct mechanism (Table 2 and Figure 4). The effect is more pronounced for methanol (0.40 and 0.26 eV for the indirect mechanism compared to 0.72 eV for the direct mechanism) although water shows a similar behavior. Therefore the molecule first dissociates onto in-plane oxygen and then the hydrogen atom is transferred to bridging oxygen. This is in accordance with a theoretical work that suggested that hydrogen from water dissociation would diffuse along bridging oxygen rows by forming intermediate hydroxyl groups on in-plane oxygen atoms.[27]

There is evidence that water readily dissociates at about 180 K.[2] Methanol, on the other hand dissociates at room temperature in seconds.[3] If we assume an Arrhenius dependence of dissociation rates with a preexponential factor of 10^{13} s^{-1}, then such a fast dissociation gives support to the indirect mechanism proposed in this work. This is also supported by the fact that the transition barriers might be underestimated in GGA[16,28] calculations increasing the direct transition barrier for methanol up to ~0.9 eV and consequently excluding dissociation in seconds at room temperature. Clearly, further experiments at several temperatures would be necessary to settle this point.

We note that the rate determining step is the first step, and the second one has a smaller transition barrier so the process would be very fast relative to the first one. It is remarkable that the use of the larger 4 × 2 supercell increases the transition barrier for the second step although it is not determining in either case. In consequence, it would be difficult to directly detect OH_{in} on the surface. This is an example of how theory complements the experimental work. Furthermore, the reverse reaction, passing from dissociated to molecular state would be highly improbable.

For the water molecule, energy differences between the direct and the indirect mechanism are smaller. This suggests that the higher energy barrier in the direct process for methanol could be due to the fact that the bulky methyl group hinders the hydroxyl from rotating. This effect might be enhanced in the dissociation of larger alcohol molecules. It is worth pointing out, that since we are interested in reaction rates we should have in mind also attempt frequencies. MD simulations show that the water molecule adopts a rigid position on the vacancy, perpendicular to the (001) direction and vibrates in such a way that the O−H bond stretches in the direction of an in-plane oxygen. Furthermore, rotations of the molecule permitting the hydrogen atom to point to nearby bridging oxygen atoms were not observed. This is the same behavior reported previously for methanol.[5] For this reason, we speculate that despite the transition barriers for both mechanisms are similar it would be more probable for water to dissociate through the indirect mechanism.

Energy profiles that represent the minimum energy path between the initial and final states are presented in Figure 4 and some optimized geometrical parameters for the transition state geometries (Figure 1 and 2) are presented in Tables S1 and S2 (Supporting Information). In general, the transition state corresponds to geometries in which the hydrogen atom is between the initial and the final configuration.

For the sake of comparison we performed additional calculations on the stoichiometric surface for the six layers and 4 × 1 supercell (Figure 3 and Tables 1 and S3). For methanol the molecular state is nearly degenerate to the dissociated state on the bridging oxygen. In contrast, the molecular state in the case of water is slightly favored (0.14 eV). This is in agreement with previous theoretical work that reported small energy differences (ca. 0.1 eV) between the molecular and the dissociated states[15−17] although the most stable was dependent on technical parameters.

Transition barriers for the direct mechanism are small (Table 2). This compares well with previous calculated values for water.[15,16] Such small barriers imply that the molecules should dissociate even at low temperatures. However, since both the direct and reverse reactions are feasible the molecule would be continually forming and breaking. It has been suggested that the energy barriers for hydroxyl diffusion on the surface are high and the dissociation will never be effective because the fragments could easily recombine to form water molecules. This process has previously been named "pseudodissociation".[15] In contrast, dissociation onto in-plane oxygen atoms is not energetically favorable since the intermediate state is energetically inaccessible (ca. 0.7 eV higher in energy) and consequently the two step mechanism is not longer valid.

In conclusion, methanol and water dissociation on defective TiO_2 (110) surfaces is promoted by in-plane oxygen atoms. The role of different surface oxygen is therefore clarified. Bridging oxygen atoms are easily removed to produce vacancies that act as preferential adsorption sites. In-plane oxygen atoms that were previously considered to play a negligible role are found to be essential as intermediate sites for dissociation. This is another example of the extraordinary complexity of surface dynamics. This behavior might be extrapolated to other molecular dis-

sociations. We expect the present study stimulates further experimental work in order to detect the intermediate OH_{in} groups on the surface. On the stoichiometric surface, dissociation is energetically feasible even at low temperatures although dissociation is not permanent since the molecules can recombine easily; the indirect mechanism is not possible in this case.

Acknowledgment. This work was funded by the Ministerio de Educación y Ciencia, MEC, from Spain (project MAT2008-09918), and the Junta de Andalucía, JA, (Project FQM-01126). R.S.A. also gratefully acknowledges the JA for a predoctoral grant. We also thank the computational resources provided by the Barcelona Supercomputing Center−Centro Nacional de Supercomputación (Spain). Dedicated to the memory of our beloved colleague and friend Lorenzo Pueyo who recently passed away.

Supporting Information Available: Optimized geometrical parameters for the transition state geometries described in the text. This material is available free of charge via the Internet at http://pubs.acs.org.

References and Notes

(1) Diebold, U. *Surf. Sci. Rep.* **2003**, *48*, 53.
(2) Wendt, S.; Matthiesen, J.; Schaub, R.; Vestergaard, E. K.; Laegsgaard, E.; Besenbacher, F.; Hammer, B. *Phys. Rev. Lett.* **2006**, *96*, 066107.
(3) Zhang, Z.; Bondarchuk, O.; White, J. M.; Kay, B. D.; Dohnálek, Z. *J. Am. Chem. Soc.* **2006**, *128*, 4198.
(4) Bikondoa, O.; Pang, C. L.; Ithnin, R.; Muryn, C. A.; Onishi, H.; Thornton, G. *Nat. Mater.* **2006**, *5*, 189.
(5) Sánchez de Armas, R.; Oviedo, J.; San Miguel, M. A.; Sanz, J. F. *J. Phys. Chem. C* **2007**, *111*, 10023.
(6) Zhang, Z.; Bondarchuk, O.; Kay, B. D.; White, J. M.; Dohnálek, Z. *J. Phys. Chem. C* **2007**, *111*, 3021.
(7) Bondarchuk, O.; Kim, Y. K.; White, J. M.; Kim, J.; Kay, B. D.; Dohnálek, Z. *J. Phys. Chem. C* **2007**, *111*, 11059.
(8) Farfan-Arribas, E.; Madix, R. J. *Surf. Sci.* **2003**, *544*, 241.
(9) Farfan-Arribas, E.; Madix, R. J. *J. Phys. Chem. B* **2002**, *106*, 10680.
(10) Brinkley, D.; Engel, T. *J. Phys. Chem. B* **2000**, *104*, 9836.
(11) Henderson, M. A.; Otero-Tapia, S.; Castro, M. E. *Faraday Discuss.* **1999**, *114*, 313.
(12) Bates, S. P.; Gillan, M. J.; Kresse, G. *J. Phys. Chem. B* **1998**, *102*, 2017.
(13) Gamble, L.; Jung, L. S.; Campbell, C. T. *Surf. Sci.* **1996**, *348*, 1.
(14) Kim, K. S.; Barteau, M. A. *Surf. Sci.* **1989**, *223*, 13.
(15) Wendt, S.; Schaub, R.; Matthiesen, J.; Vestergaard, E. K.; Wahlström, E.; Rasmussen, M. D.; Thostrup, P.; Molina, L. M.; Laegsgaard, E.; Stensgaard, I.; Hammer, B.; Besenbacher, F. *Surf. Sci.* **2005**, *598*, 226.
(16) Lindan, P. J. D.; Zhang, C. *Phys. Rev. B* **2005**, *72*, 075439.
(17) Harris, L. A.; Quong, A. *Phys. Rev. Lett.* **2004**, *93*, 086105.
(18) Pang, C. L.; Sasahara, A.; Onishi, H.; Chen, Q.; Thornton, G. *Phys. Rev. B* **2006**, *74*, 073411.
(19) Zhang, Z.; Bondarchuk, O.; Kay, B. D.; White, J. M.; Dohnálek, Z. *J. Phys. Chem. B* **2006**, *110*, 21840.
(20) Kresse, G.; Joubert, J. *Phys. Rev. B* **1999**, *59*, 1758.
(21) Perdew, J. P.; Chevary, J. A.; Vosko, S. H.; Jackson, K. A.; Pederson, M. R.; Singh, D. J.; Fiolhais, C. *Phys. Rev. B* **1992**, *46*, 6671.
(22) Kresse, G.; Furthmuller, J. VASP, the Guide; http://cms.mpi-.univie.ac.at/vasp/vasp/vasp.html.
(23) Oviedo, J.; San Miguel, M. A.; Sanz, J. F. *J. Chem. Phys.* **2004**, *121*, 7427.
(24) Monkhorst, H.; Pack, J. *Phys. Rev. B* **1976**, *13*, 5188.
(25) Mills, G.; Jónsson, H.; Schenter, G. K. *Surf. Sci.* **1995**, *324*, 305.
(26) Henkelman, G.; Uberuaga, B. P.; Jónsson, H. *J. Chem. Phys.* **2000**, *113*, 9901.
(27) Kajita, S.; Minato, T.; Kato, H. S.; Kawai, M.; Nakayama, T. *J. Chem. Phys.* **2007**, *127*, 104709.
(28) Zhang, Y.; Yang, W. *J. Chem. Phys.* **1998**, *109*, 2604.

JP805759Y